Table I. Electroreduction of O_2 in Acetonitrile at Platinum or at Glassy Carbon Electrodes

A. Singlet Oxygen Yields at a Platinum Cathode[a]

sample	singlet oxygen yield[b,c] (mol/faraday of electrolysis) experimental	theoretical
0.1 M $HClO_4$	0.08 ± 0.03	0.5 (0.15)[e]
0.1 M $Et_4N(ClO_4)$[d]	0.004 ± 0.003	

B. Yield of $^{34}(O_2)$[j]

sample (71 μmol) 50:50	$I_{34}/(I_{34}+I_{36})$ MS analysis	calcd[f]
$^{36}(O_2)$ standard	0.04 ± 0.01	
product gas from 104 μmol electrolysis ($1e^-/O_2$) at Pt	0.20 ± 0.01	0.69 (0.20)[g]
product gas from 21 μmol electrolysis ($1e^-/O_2$) at GC	0.16 ± 0.01	0.20[h]

C. Yield of Dibenzoyl Benzene (DBB)[k]

sample (O_2, 1 atm)	yield of DBB, μmol[i]
product from 32 μmol electrolysis ($1e^-/O_2$)	4 ± 1 (25% conversion efficiency)

[a] Estimated from the intensity of the 1268-nm light emission during steady-state electrolysis. 8 mM O_2 (1 atm), two-electrode cell (both platinum), and 3-V applied potential. Emission studies were not attempted with glassy carbon electrodes. [b] Singlet oxygen yields were estimated from the integrated intensity of the 1268-nm emission for the (H_2O_2 + HOCl) reaction (in ^2H_2O solvent) as a standard source of $^1O_2$. The yields have been corrected for the longer lifetime of $^1O_2$ in acetonitrile (65 μs) compared to ^2H_2O (58 μs), but no correction was applied for quenching by $HO_2^\bullet$. [c] Spectral analysis of emission band: 1070-nm filter, −0.01 ± 0.01; 1170-nm, 0.02 ± 0.01; 1268-nm, 1.00 ± 0.05; 1375-nm, 0.21 ± 0.01; 1470 nm, 0.03 ± 0.01; 1580-nm, 0.03 ± 0.01 (ref 3). [d] Control sample without a source of H^+. [e] The theoretical yield assuming an electrolysis efficiency of 29.0% for $O_2 + e^- + H^+ \rightarrow HOO^\bullet$ is 0.15. [f] Assuming 2[50:50 $^{36}(O_2)$:$^{32}(O_2)$] + $2H^+ + 2e^- \rightarrow$ [2 $HOO^\bullet$] → [HOOOOH] → O_2 + HOOH is the only reaction pathway, product should be 25% $^{32}O_2$, 50% $^{34}O_2$, and 25% $^{36}O_2$. This gives a value of 0.67 for $[I_{34}/(I_{34}+I_{36})]$, but the original $^{36}O_2$ had an assay of 0.045 for this quantity (ref 4). [g] Calculated value for an estimated electrolysis efficiency of 29.0% for $O_2 + e^- + H^+ \rightarrow HOO^\bullet$; remaining current at Pt produces H_2 ($2H^+ + 2e^- \rightarrow H_2$). Estimate based upon the ratio of the electrolysis current density at a GC electrode relative to that at a Pt electrode $[(i_{GC}/i_{Pt})100]$. [h] Calculated on the basis that 21 μmol of $HOO^\bullet$ are formed to give 10.5 μmol of O_2[52.2% $^{34}(O_2)$ and 23.9% $^{36}(O_2)$]; this plus the remaining 50 μmol of O_2 [2.2% $^{34}(O_2)$ and 47.8% $^{36}(O_2)$] gives a value of 0.20 for $[I_{34}/(I_{34}+I_{36})]$. [i] Assayed by capillary-column gas chromatography. [j] From the electrolysis of a 50:50 $^{36}(O_2)$:$^{32}(O_2)$ mixture (0.33 atm O_2, 0.67 atm Ar) in acetonitrile (0.1 M $HClO_4$). [k] From the electrolysis of O_2 at GCE in the presence of 3 mM diphenylisobenzofuran (DPBF) (0.1 M NH_4ClO_4 in place of 0.1 M $HClO_4$).

$HOO^\bullet$ systems is small. Combination of 12 mM $O_2^{\bullet-}$ [$(Me_4N)O_2$ dissolved in dimethylformamide (DMF)][7] with an equal volume of 100 mM $HClO_4$ in DMF (in the spectrometer cuvet) yields approximately 1.5 μM $^1O_2$ [0.05% of the total O_2 produced ($2HOO^\bullet \rightarrow O_2 + HOOH$) on the basis of its integrated 1268-nm chemiluminescence].[8] When this experiment is conducted in acetonitrile, the yield of $^1O_2$ is a factor of 40 smaller (but still with a signal-to-noise ratio greater than 10). In the absence of protons, $O_2^{\bullet-}$ solutions do not give a detectable emission at 1268 nm. These yields of $^1O_2$ are so small that they may have resulted from an unknown side reaction rather than the process of eq 1.

Scheme I outlines self-consistent decomposition pathways for the perhydroxyl radical ($HOO^\bullet$) that are in accord with the experimental results. The heterogeneous production of $HOO^\bullet$ at an electrode surface [pathway (a)] appears to give oriented molecules with the H-ends at the electrode surface, such that their radical ends are in close proximity for radical–radical coupling. In contrast, the homogeneous production of $HOO^\bullet$ from the addition of superoxide to excess protons [pathway (b)] affords conditions under which it can decompose to HOOH and O_2 by three routes: (1) Electron transfer from residual $O_2^{\bullet-}$ to $HOO^\bullet$, which is dominant in all but the most extreme conditions and only yields $^3O_2$;[9,10] (2) Hydrogen-atom transfer from one $HOO^\bullet$ to another via head-to-tail coupling, which is favored in nonbasic solvents such as acetonitrile (and in the gas phase)[11] and only yields $^3O_2$; and (3) Radical–radical coupling of two $HOO^\bullet$ groups, which is favored to a limited extent in basic solvents that inhibit head-to-tail coupling and can yield $^1O_2$.

Acknowledgment. This work was supported by the National Science Foundation under Grant CHE-8516247 (D.T.S.), by the Welch Foundation under Grant A-1042 (D.T.S.), by the National Institutes of Health under Grant GM 32974 (J.R.K.), by the Veterans Administration Research Service (J.R.K.), and by a grant from the Potts Estate (administered by Loyola Unversity Stritch School of Medicine) (J.R.K.).

(7) Tetramethylammonium superoxide was synthesized and assayed via established methods (Sawyer, D. T.; Calderwood, T. S.; Yamaguchi, K.; Angelis, C. T. *Inorg. Chem.* **1983**, *22*, 2577–2583).

(8) The H_2O_2 + HOCl reaction (^2H_2O solvent) was used as a $^1O_2$ standard. These yields have been corrected for the $^1O_2$ oxygen lifetime in the solvent ([DMF, 16 μs (J.R.K., unpublished); MeCN, 65 μs; ^2H_2O, 58 μs] but not for quenching by ^2H_2O. These estimates thus represent a lower limit for the $^1O_2$ yield.

(9) Andrieux, C. P.; Hapiot, P.; Saveant, J.-M. *J. Am. Chem. Soc.* **1987**, *109*, 3768–3775.
(10) Roberts, J. L., Jr.; Sawyer, D. T. *Isr. J. Chem.* **1983**, *23*, 430–438.
(11) Niki, H.; Maker, P. D.; Savage, C. M.; Breitenback, L. P. *Chem. Phys. Lett.* **1980**, *73*, 43.

Surface Photochemistry. 4. Quenching of Methyl Iodide on Pt(111)

Z.-M. Liu, S. Akhter, B. Roop, and J. M. White*

Department of Chemistry, University of Texas Austin, Texas 78712

Received July 8, 1988

The surface photochemistry of small adsorbed molecules is, in several cases, competitive with quenching of excited electronic states on both metals and nonmetals.[1-15] On Pt(111), the results for CH_3Br and CH_3Cl[2,3] suggest that CH_3X (X = Br, Cl) absorbs UV light and forms a repulsive excited state and, with significant probability, that the C–X bond cleaves even though other relaxation paths exist.[16,17] Since these two methyl halides show

(1) Roop, B.; Costello, S. A.; Greenlief, C. M.; White, J. M. *Chem. Phys. Lett.* **1988**, *143*, 38.
(2) Costello, S. A.; Roop, B.; Liu, Z.-M.; White, J. M. *J. Phys. Chem.* **1988**, *92*, 1019.
(3) Zhou, Y.; Feng, W. M.; Henderson, M. A.; Roop, B.; White, J. M. *J. Am. Chem. Soc.* **1988**, *110*, 4447.
(4) Grassian, V. H.; Pimentel, G. C. *J. Chem. Phys.* **1988**, *88*, 4478 and 4484.
(5) Bourdon, E. B. D.; Cowin, J. P.; Harrison, I.; Polanyi, J. C.; Segner, J.; Stanners, C. D.; Young, P. A. *J. Phys. Chem.* **1984**, *88*, 6100.
(6) Bourdon, E. B. D.; Das, P.; Harrison, I.; Polanyi, J. C.; Segner, J.; Stanners, C. D.; Williams, R. J.; Young, P. A. *Faraday Discuss. Chem. Soc.* **1986**, *82*, 343.
(7) Marsh, E. P.; Tabares, F. L.; Schneider, M. R.; Cowin, J. P. *J. Vac. Sci. Technol.* **1987**, *A5*, 519.
(8) Tabares, F. L.; Marsh, E. P.; Bach, G. A.; Cowin, J. P. *J. Chem. Phys.* **1987**, *86*, 738.
(9) Chuang, T. J. *Surf. Sci.* **1986**, *178*, 763.
(10) Chuang, T. J.; Domen, K. *J. Vac. Sci. Technol.* **1987**, *A5*, 473.
(11) Domen, K.; Chuang, T. J. *phys. Rev. Lett.* **1987**, *59*, 1484.
(12) Celii, F. G.; Whitmore, P. M.; Janda, K. C. *Chem. Phys. Lett.* **1987**, *138*, 257.
(13) Ying, Z.; Ho, W. *Phys. Rev. Lett.* **1988**, *60*, 57.
(14) Marsh, E. P.; Schneider, M. R.; Gilton, T. L.; Tabares, F. L.; Meier, W.; Cowin, J. P. *Phys. Rev. Lett.* **1988**, *60*, 2551.
(15) Domen, K.; Chuang, T. J. *J. Chem. Phys.* Submitted for publication.

0002-7863/88/1510-8708$01.50/0

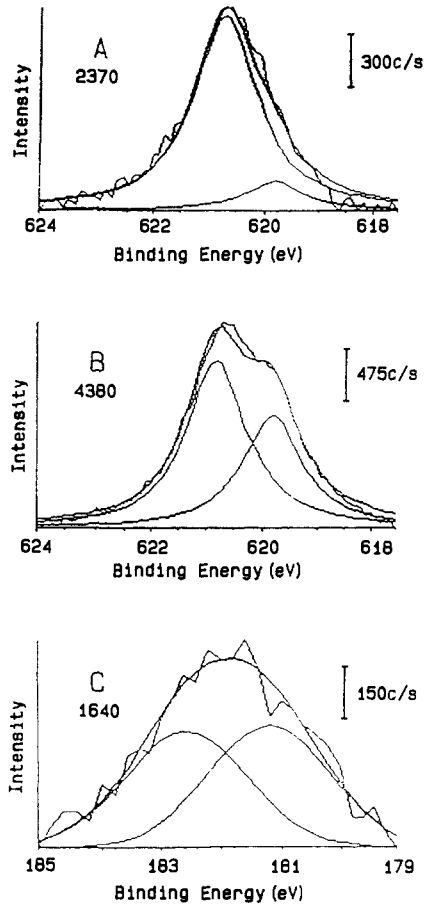

Figure 1. Core level spectra of halogen regions after photolysis. The noisy spectra are the raw XPS data. The smooth curves are synthesized fits using Gaussian and Lorentzian profiles. (A) I(3d) spectrum for monolayer CH_3I on Pt(111) and photolyzed for 2 h with a 100-W Hg arc. (B) I(3d) spectrum for 1.85 ML of CH_3I photolyzed for 2 h. (C) Br(3p) spectrum for monolayer CH_3Br photolyzed for 1 h. I(3d) spectra were taken at 40 eV and Br(3p) spectra at 80 eV pass energy. The numbers beneath the panel labels are the integrated peak areas. The Br signal is much weaker than the I signal because its photoionization cross section is much lower.

no thermal chemistry on Pt(111) it is easy to distinguish the role of photochemistry. By contrast, CH_3I adsorbs molecularly at 100 K, but a large fraction thermally decomposes between 200 and 250 K.[18]

In this communication, we report on CH_3Br and CH_3I surface photochemistry on Pt(111), by using core level X-ray photoelectron spectroscopy (XPS) to distinguish halogens bound and not bound to C. Thermal decomposition of CH_3I is avoided by keeping the temperature below 120 K during photolysis and analysis. The XPS spectra, with and without UV irradiation, were recorded with a Kratos Series 800 system that includes a hemispherical analyzer and Mg Kα radiation (1253.6 eV, 300 W). Purified CH_3Br or CH_3I was dosed onto a clean Pt(111) surface at 106–110 K. By using an established, reproducible procedure,[18] monolayer (ML) coverages were produced by dosing multilayers and removing the latter by warming. For CH_3I, multilayer desorption peaks at 140 K, and the undecomposed part of the monolayer peaks at 239 K.[18] For CH_3Br, the analogous peaks are at 164 and 126 K.[18]

The samples were illuminated through a quartz vacuum window with a focussed, quartz bulb, 100-W Hg arc that has significant intensity only above 250 nm.[19] The incident power was 0.09 ± 0.01 W, and the temperature reached during irradiation never exceeded 119 K.

Figure 1 shows the XPS core level spectra of the I(3d) and Br(3p) regions *after* photolysis. In the absence of irradiation but after a 2-h waiting period, the I(3d) spectrum can be fit with a single peak at 620.8 ± 0.1 eV BE and a FWHM of 1.3 eV. Irradiating monolayer CH_3I for 2 h leads to an asymmetric spectrum that can be fit with two components of 1.3 eV half-width centered at 620.8 and 619.8 ± 0.1 eV BE, respectively (Figure 1A). The low BE peak contributes 12% (0.1 ML) of the total area. There was no loss of I(3d) or C(1s) intensity due to irradiation. The low BE is equal to that measured for adsorbed I atoms in our apparatus and for metal iodides (619.5 ± 0.2 eV).[20] The higher BE component is attributed to molecularly adsorbed CH_3I. The Pt ($4f_{7/2}$) BE was 70.9 eV throughout these experiments.[20]

For 1.85 ML of CH_3I photolyzed for 2 h (Figure 1B), the same two peaks (620.8 and 619.8 eV BE and 1.3 eV FWHM) appear, but the low BE peak is more than seven times as intense (0.75 ML) as for the monolayer. For both CH_3I coverages, the X-ray flux caused negligible photochemistry.

Figure 1C shows the spectra for monolayer CH_3Br. In the absence of irradiation but after waiting 1 h, the Br(3p) spectrum is readily fit with a single peak centered at 182.5 ± 0.2 eV BE and 2.4 eV FWHM. After 1-h irradiation, the peak is much broader (Figure 1C) but can be fit with two peaks of 2.4 eV FWHM centered at 182.5 and 181.1 ± 0.2 eV, respectively. The latter is the same as for Br on Pt.[21] Each peak contributes about 50% (0.5 ML) to the total area indicating much more efficient photolysis than for the monolayer iodide. There is a very small loss of Br(3p) and C(1s) intensity during irradiation, but this is fully accounted for by slow thermal desorption.[21]

There are two major points to be made from these results: (1) Monolayer CH_3I is photolyzed much less readily than monolayer CH_3Br and (2) multilayer CH_3I is photolyzed much more readily than monolayer CH_3I. We interpret these results as indicating significantly stronger quenching by the Pt(111) substrate of the monolayer CH_3I than either the monolayer CH_3Br or the multilayer CH_3I.

Throughout the region above 250 nm, where the Hg arc has significant intensity, the gas and solution phase bromide and iodide have (1) continuous and unstructured absorption spectra, (2) optical absorption cross sections favoring the iodide by at least 2 orders of magnitude at every wavelength, and (3) photodissociation quantum yields near unity.[22,23] On the basis of physisorption models and our XPS data, we estimate that the surface concentration of monolayer CH_3I is less, but within 20%, than monolayer CH_3Br. Thus, if the gas-phase properties extended to the surface, monolayer CH_3I would be more efficiently photolyzed than monolayer CH_3Br, but just the opposite is observed (Figure 1 (parts A and C)). Since surface vibrational spectra indicate weakly perturbed, adsorbed ground state, parent molecules,[18] we propose that the low yield of C–I bond cleavage is the result of very rapid quenching of the excited state and that this is due to slightly stronger bonding of CH_3I with Pt(111). Stronger bonding is evidenced by the monolayer TPD peaks (239 vs 164 K).

That quenching is strongly dependent on proximity to the surface is evident in the 1.85 ML experiment with CH_3I. Our results indicate that all of the molecules in excess of the monolayer are readily photolyzed (90% of second layer decomposed in Figure 1B). Even in the second layer, this I finds itself close enough and moving slowly enough to be captured.

On the basis of the incident energy and on the initial rate of conversion, we can estimate the number of molecules decomposed

(16) Campion, A.; Gato, A. R.; Harris, C. B.; Robota, H. J.; Whitmore, P. M. *Chem. Phys. Lett.* **1980**, *73*, 447.
(17) Avouris, P.; Persson, B. N. J. *J. Phys. Chem.* **1984**, *88*, 837.
(18) Henderson, M. A.; Mitchell, G. E.; White, J. M. *Surf. Sci.* **1987**, *184*, L325.
(19) White, J. M. Ph.D. Dissertation, University of Illinois, 1966.
(20) Wagner, C. D.; Riggs, W. M.; Davis, L. E.; Moulder, J. F.; Mullenberg, G. E. *Handbook of X-ray Photoelectron Spectroscopy*; Perkin-Elmer: Eden Prairie, MN, 1979.
(21) Roop, B.; Lloyd, K.; Liu, Z.-M.; White, J. M. to be published.
(22) Calvert, J. C.; Pitts, J. N. *Photochemistry*; Wiley: New York, 1966.
(23) Okabe, H. *Photochemistry of Small Molecules*; Wiley: New York, 1978.

per incident photon. Assuming an average energy corresponding to a wavelength of 320 nm, we estimate 1.4×10^{-7} and 1.0×10^{-8} molecules/incident photon for CH_3Br and CH_3I. Because the photon absorption cross section is unknown, we cannot estimate quantum yields.

Acknowledgment. This work was supported in part by the National Science Foundation Grant CHE 8505413.

Kinetic Studies of the Sphere–Rod Transition of Micelles

Shoji Harada,* Nobuya Fujita, and Takayuki Sano

Department of Materials Science, Faculty of Science, Hiroshima University Naka-ku, Hiroshima 730, Japan

Received May 11, 1988

Some surfactants change their micellar shape from sphere to rodlike by an increase of concentration or by the addition of electrolytes.[1] The sphere–rod transition of micelles has been widely studied, but no kinetic experiment has been done, and the mechanism of the transition has not been clarified. In this work, we studied the sphere–rod transition of cetyltrimethylammonium bromide (CTAB) micelle both statically and kinetically and reached a conclusion that the rodlike micelle is formed by successive association of the monomers to the sphere micelles.

The aggregation behaviors of CTAB were studied by conductivity and ultrasonic velocity measurements. In the plots of these properties against the CTAB concentration, a break point was observed at 1.0 mM, which was ascribed to the CMC.[2] As seen in Figure 1, another break point was observed at around 250 mM, which is in accordance with the reported value for the sphere–rod transition concentration of CTAB micelle.[3] In contrast to these, the plots for the cetyltrimethylammonium chloride (CTAC) solution where the micellar shape remains unchanged were linear, and any break point was not observed.

Pressure-jump studies were performed on the CTAB solution in a wide concentration range. In a solution of concentration a little above the CMC, two relaxations were observed. Temperature dependencies of their reciprocal relaxation times are shown in Figure 2 where we can observe that they are similar to those for other surfactants.[4] Following preceding studies[5] the fast relaxation with a time constant of about 10 ms might be ascribed to the monomer exchange and the slow relaxation with a time constant of about 1 s to the overall formation and dissolution of the sphere micelles. The relaxation amplitudes and the relaxation times reduced with an increase of CTAB concentration, and the relaxations were not observed in a concentration range of about 20–230 mM. As the CTAB concentration approaches the sphere–rod transition concentration (250 mM), two new relaxations appeared. These relaxations could be induced even in 200 mM CTAB solution by the addition of 20 mM NaBr to decrease the sphere–rod transition concentration to 190 mM. On the other hand, no relaxation was observed in a CTAC solution. These results imply that the relaxations are related to the rodlike micelles of CTAB.

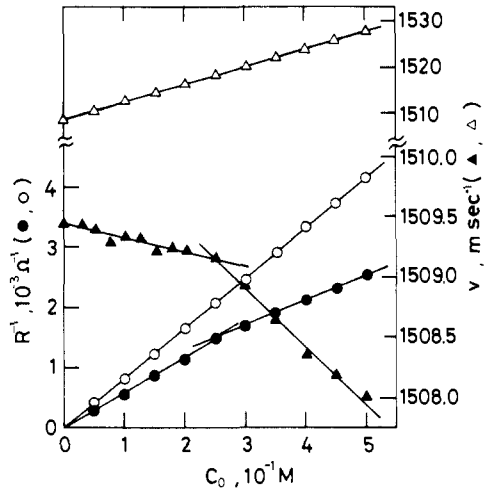

Figure 1. Concentration dependencies of the conductivity (●, ○) and the ultrasonic velocity (▲, △) for CTAB (filled signs) and CTAC (open signs) solutions at 30 °C. Experimental errors are about $4 \times 10^{-5}\ \Omega^{-1}$ and 0.15 m s^{-1}, respectively.

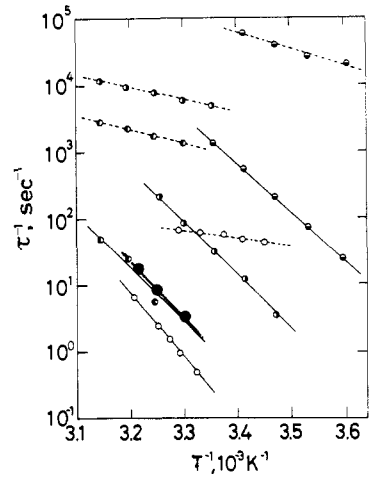

Figure 2. Temperature dependencies of the reciprocal relaxation times for the fast process (dotted line) and the slow process (full line) at a little above the CMC: (◒), 10 mM sodium dodecylsulfate; (◑), 2.4 mM sodium tetradecylsulfate; (◐), 1 mM sodium hexadecylsulfate; (○), 1.1 mM CTAB. Data for the slow relaxation in a 400 mM CTAB solution is shown by (—●—).

Detailed kinetic experiments for the CTAB solutions in the concentration range above the sphere–rod transition concentration revealed the following facts. In the fast relaxation, the reciprocal relaxation time increases linearly with CTAB concentration. In the slow relaxation, the concentration dependency of the reciprocal relaxation time τ_s^{-1} is not monotonous but rather complicated as seen in Figure 3. Another feature of the slow relaxation is an unusually large temperature dependency of the relaxation time (Figures 2 and 3). Very interestingly, these concentration and temperature dependencies of the two relaxation times are very similar to those of the relaxations observed for the sphere micelles above the CMC.[4,5] With reference to the two relaxations for the sphere micelles, the data indicate that the fast relaxation is due to the monomer exchange, while the slow relaxation is due to the overall formation and dissolution of the rodlike micelles. Furthermore, the unusually large apparent activation energy of the slow process can be well understood by considering that a rodlike micelle might be produced by the monomer's successive association

(1) (a) Husson, F. R.; Luzzati, V. *J. Phys. Chem.* **1964**, *68*, 3504. (b) Hoffmann, H.; Platz, G.; Rahage, H.; Schorr, W.; Ulbricht, W. *Ber. Bunsenges. Phys. Chem.* **1981**, *85*, 255. (c) Missel, P. J.; Mazer, N. A.; Benedek, G. B.; Carey, M. C. *J. Phys. Chem.* **1983**, *87*, 1264. (d) Imae, T.; Kamiya, R.; Ikeda, S. *J. Colloid Interface Sci.* **1985**, *108*, 215.

(2) (a) Scott, A. B.; Tarter, H. V. *J. Am. Chem. Soc.* **1943**, *65*, 692. (b) Lawrence, A. S. C.; Stenson, R. *Proceedings of the International Congress Surface Activity*, 2nd ed.; London, 1957, Vol. II, p 368. (c) Mukerjee, P.; Mysels, K. J. Critical Micelle Concentrations of Aqueous Surfactant Systems. *Nat. Stand. Ref. Data Ser. Nat. Bur. Stand. (U.S.)* **1971**, 36.

(3) (a) Ekwall, P.; Mandell, L.; Solyom, P. *J. Colloid Interface Sci.* **1971**, *35*, 519. (b) Lindblom, G.; Lindman, B.; Mandell, L. *J. Colloid Interface Sci.* **1973**, *42*, 400. (c) Ulmius, J.; Lindman, B.; Lindblom, G.; Drankenberg, T. *J. Colloid Interface Sci.* **1978**, *65*, 88.

(4) (a) Folger, R.; Hoffmann, H.; Ulbricht, W. *Ber. Bunsenges. Phys. Chem.* **1974**, *78*, 986. (b) Aniansson, E. A. G.; Wall, S. N.; Almgren, M.; Hoffmann, H.; Kielmann, I.; Ulbricht, W.; Zana, R.; Lang, J.; Tondre, C. *J. Phys. Chem.* **1976**, *80*, 905. (c) Diekmann, S. *Ber. Bunsenges. Phys. Chem.* **1979**, *83*, 528.

(5) (a) Reference 4. (b) Aniansson, E. A. G.; Wall, S. N. *J. Phys. Chem.* **1974**, *78*, 1024. (c) Teubner, M.; Diekmann, S.; Kahlweit, M. *Ber. Bunsenges. Phys. Chem.* **1978**, *82*, 1278.

0002-7863/88/1510-8710$01.50/0